JOURNAL OF MATERIALS SCIENCE 21 (1986) 1721–1729

Preferential distribution of chromium and nickel in the borided layer obtained on synthetic Fe–Cr–Ni alloys

C. BADINI, C. GIANOGLIO, G. PRADELLI
Dipartimento di Scienza dei Materiali e Ingegneria Chimica, Politecnico di Torino, Turin, Italy

Synthetic ferrous alloys containing chromium and/or nickel were prepared and borided at 1173 K with powders containing B_4C, KBF_4 and SiC for times varying from 20 to 60 h. The surface layers composed of borides of type (Fe, M)B and (Fe, M)$_2$B were characterized by means of X-ray diffraction, microscopic observations, analysis with the microprobe and microhardness measurements. A quantitative study was carried out on the differentiated distribution of chromium and nickel in the phases constituting the borided layer. The chromium spreads from the matrix towards the borided layer, where it is concentrated in the phase richest in boron (Fe, M)B. Nickel behaves in the opposite manner. Alloys without carbon were used in order to avoid the formation of an area containing carbides and boron carbides, situated between the borided layer and the matrix, which could influence chromium distribution. The distribution phenomenon is in accordance with what was found in the study of Fe–M–B ternary systems (M = Cr, Ni). The influence of chromium and nickel on the thickness, the morphology and the microhardness of the borided layer are discussed.

1. Introduction

It is well known that the thermal treatment of boriding carried out on steels makes it possible to obtain, outside a metallic object, a diffusion layer of considerable hardness (up to $\sim 21\,kN\,mm^{-2}$) [1], which is very hard-wearing. This layer is predominantly composed of phases of the type FeB (rhombic) and Fe_2B (tetragonal), which are in reality solid solutions of formula (Fe, M)B and (Fe, M)$_2$B (M = Cr, Mn, Ni, Co, Mo, . . .). The morphology and hardness of the borided layer depend on the composition of the alloy treated, since the borides FeB and Fe_2B are capable of dissolving even considerable quantities of transition metals, as we pointed out in the course of a great deal of preliminary research work into systems Fe–M–B (M = Cr, Mn, Ni, Co) [2–5].

In the course of a study aiming to define the distribution of the elements in an alloy between the phases which constitute the borided layer obtained on ferrous alloys, in a recent paper [6] we reported the preliminary results regarding the distribution of chromium and nickel between the phases (Fe, M)B and (Fe, M)$_2$B present in the diffusion layer of chromium and nickel steels of the type AISI 430 and AISI 304. In particular, it was found that chromium spreads from the matrix towards the borided layer and that here it is preferentially and systematically distributed in the outermost phase constituted by (Fe, M)B. Nickel, on the other hand, tends to concentrate in the middle area between the matrix and the borided layer, and inside this it inserts itself preferentially into the tetragonal boride. In the middle area between the matrix and the diffusion layer, as confirmed by several authors [7–9], boron carbides of formula (Fe, M)$_3$(B, C), (Fe, M)$_{23}$(B, C)$_6$ and (Fe, M)$_7$(B, C)$_3$ are present, derived by substitution Fe–M or Cr–M in the carbides Fe_3C, $Cr_{23}C_6$ and Cr_7C_3.

The results obtained regarding the distribution of chromium and nickel betweeen the phases (Fe, M)B and (Fe, M)$_2$B existing in the diffusion layer are in agreement with the findings of the study of two-phase fields of systems Fe–Cr–B [10] and Fe–Ni–B [4]. It is therefore confirmed that also in the diffusion layer obtained on steels the metallic element with the lower atomic number is preferentially inserted into the phase (Fe, M)$_2$B which is poorer in boron and that, on the contrary, the one with higher atomic number is concentrated in the rhombic phase (Fe, M)B.

This behaviour, observed in numerous ternary systems constituted of boron and transition elements, is of a general character and is the subject of one of our previous papers [11].

The presence of boron carbides crystals in the middle area, in considerable quantities in steels with a high carbon content, slows down the diffusion of chromium from the matrix to the outer layer because of the latter element's tendency to enter into a solid solution in the above-mentioned phases.

The limited extent of the interface between the phases (Fe, M)B and (Fe, M)$_2$B together with its continuous advancement contributes in addition to preventing the equilibrium conditions from being reached in borided alloys, whereas these conditions are obtained on powder samples.

Literature does not report results of studies about the boriding of ferrous alloys with no carbon [12].

0022–2461/86 $03.00 + .12

Therefore, in this study we worked on a series of metallic Fe–Cr–Ni alloys in order to define chromium and nickel distribution between the phases (Fe, M)B and $(Fe, M)_2B$ and between the latter and the matrix in the absence of carbon and therefore in the absence of the middle area of accumulation of boron carbides.

We believe that the results obtained in the course of this research can also provide positive contributions to the correct interpretation of the effect of carbon on the morphology and hardness of the phases which make up the borided layer. Indeed in literature the interpretations do not always coincide [8, 13, 14] with regard to the position of carbon between the matrix and the borided layer and to the consequences derived from the presence of this element on the morphology and hardness of the diffusion layer.

2. Methods of sample preparation and characterization

The Fe–Cr, Fe–Ni and Fe–Cr–Ni alloys prepared for this research, whose composition is reported in Table I, were obtained from Merck reduced iron (Fe > 99.5 wt %), ICN K & K chromium (Cr = 99.9 wt %) and Merck nickel (Ni > 99.5 wt %). The powder mixtures, with a particle size lower then 10 μm, homogenized and formed with a press operating at a pressure of 200 MPa into tablets weighing 10g, were melted in an arc furnace in an inert atmosphere (argon T, P = 150 mm Hg).

The homogeneity of the alloys was obtained by the remelting of the samples.

The boriding treatment was carried out at 1173 K (900° C) for times ranging from 20 to 60 h, inserting the alloys into ceramic containers with boriding powders of appropriate composition in order to obtain similar thicknesses for the two phases (Fe, M)B and $(Fe, M)_2B$.

The treatment time was lengthened in order to allow the diffusion processes to occur.

Another series of samples of the alloys examined was also treated keeping temperature, time and composition of the boriding agent constant in order to be able to carry out correctly comparisons regarding the thickness and morphology of the diffusion layers.

The boriding powders were obtained by mixing B_4C Fluka AG (7.5–40 wt %), KBF_4 Fluka AG (2.5–10 wt %) and SiC Carlo Erba (50–90 wt %). The containers were sealed with a layer of sodium silicate pentahydrate, which, melting at a temperature of 350–353 K (77–80° C), made it possible to keep the reactive atmosphere around the specimens and to avoid contact with the air. In order to facilitate the diffusion of the boron, the surfaces of the specimens, previously lapped, were degreased before the treatment.

In the course of the preparation of the specimens for metallographic analysis, in order to avoid damaging the borided layer, a thin layer of melted zinc was deposited on the surface of the specimens. The samples were transected by a slow microcutting-off machine equipped with a diamond wheel.

The hardness values of the phases constituting the borided layer were obtained with a Vickers microdurometer (load 1 and 2N). The values obtained are the results of an average of at least 12 measurements. The identification of the phases present in the borided layer was carried out by means of X-ray diffraction, subjecting the samples to analysis after the progressive removal of measured thicknesses of material.

Observation through the scanning electron microscope was carried out on samples not chemically etched since the etch reagent causes a selective dissolution of some constituents, so modifying the differentiated distribution of the metallic elements. It was therefore necessary to exploit the phase contrast appropriately in order to differentiate adequately the phases present in the diffusion layer.

An energy dispersive spectrometer was used for the microanalysis. The percentages of transition metals present in the borides of the diffusion layer were obtained, as was explained in detail earlier [6], by analysing rectangular shaped areas (5 μm × 60 μm), adjacent to each other and positioned perpendicularly to the edge of the sample.

For the transition areas, in which there is a reciprocal penetration of phases in contact, analyses were carried out on areas of limited size (3 μm × 25 μm) in order to show better the variation of metallic atom concentrations with the depth.

TABLE I

Type of alloy				Treatment conditions at 1173 K			
Sample no.	Composition (wt %)			Composition of the boriding powders (wt %)			Treatment time (h)
	Fe	Cr	Ni	B_4C	KBF_4	SiC	
1	100	–	–	30	5	65	24
2	92	–	8	30	5	65	24
3	92	–	8	40	10	50	24
4	92	–	8	7.5	2.5	90	24
5	82	–	18	30	5	65	24
6	82	–	18	40	10	50	48
7	92	8	–	30	5	65	24
8	92	8	–	7.5	2.5	90	24
9	82	18	–	30	5	65	24
10	82	18	–	20	5	75	60
11	74	18	8	30	5	65	24
12	74	18	8	40	10	50	20

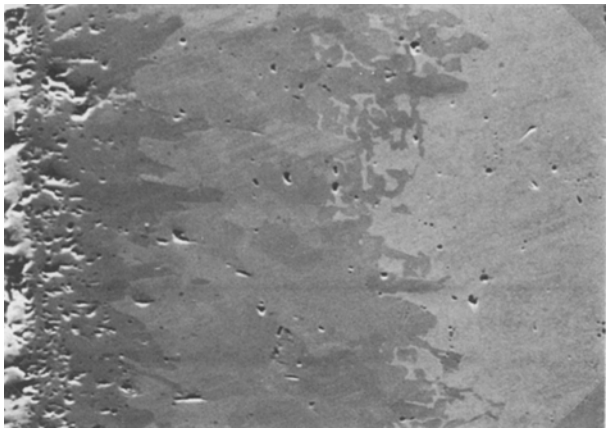

Figure 1 Sample No. 2, not etched, 350X.

3. Results and discussion

Using the previously indicated methods, specimens of Fe–Cr, Fe–Ni and Fe–Cr–Ni alloys were borided, appropriately varying the length of treatment at 1123 K (900° C) and the composition of the boriding mixture (see Table I) in order to show better both the growth of the diffusion layer and the distribution of the elements in the alloy. The results are recorded in Figs 3, 6, 10–13, 16 and 17 in histograms which represent the average composition and extension of the one-phase zones present in the diffusion layer. To point out the variation of composition in the two-phase areas of the layer in which different phases penetrate together, the values of analysis carried out on limited areas are indicated with continuous lines superimposed on the histogram. From the extremities of these curves it was possible to obtain the distribution ratio value (which will subsequently be defined) for each metallic element between the adjacent phases. For examination of the borided layer obtained on an Fe–Ni alloy containing 8% nickel (Fig. 1) it can be seen that boron diffusion occurs along an advancement front which is not parallel to the edge of the specimen and that it gives rise to extremely irregular interfaces (in particular between the matrix and phase $(Fe, Ni)_2B$) with inclusions of islands of different composition inside each "one-phase" area.

The appearance of the contact surface of the borided layers is comparable with that of the samples of Armco iron treated in the same conditions (Fig. 2) whereas the thickness of the layer is smaller.

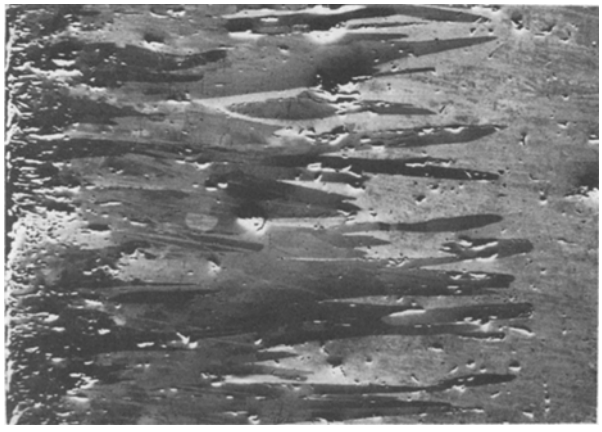

Figure 2 Sample No. 1, not etched, 210X.

The diffusion layer obtained on the Fe–Ni alloy containing 8% nickel (Fig. 3) is composed of an external phase (Fe, Ni)B with an average nickel content of about 5% and a layer which belongs to the phase $(Fe, Ni)_2B$ with a nickel content similar to that of the borided alloy. On the edge of the sample and between the layer of $(Fe, Ni)_2B$ and the matrix an accumulation of nickel was found, as already seen in the case of borided nickel steel. In the Fe–Ni alloy containing 18% nickel the diffusion layer is less deep compared with that obtained in an alloy containing only 8% nickel borided in the same conditions. The interfacial areas included between the layers (Fe, Ni)B and $(Fe, Ni)_2B$ and between the latter and the matrix (Figs. 4 and 5) are also less thick and less indented.

The analysis of the diffration patterns, carried out on the surface of this specimen shows a slightly preferred orientation of the borided crystals which tend to position themselves with the z-axis parallel to the direction of boron diffusion.

Fig. 6 shows the average nickel concentration profiles and the nickel interface concentration profiles observed on the sample containing 18% of this element.

It seems clear from the comparison of Figs. 7 and 8 with those regarding the Fe–Ni alloys that the presence of chromium slows down the diffusion of boron considerably and consequently makes it possible to obtain borided layers which are thinner than those which, in the same working conditions, are achieved on specimens of Armco iron or on Fe–Ni alloys.

In the Fe–Cr sample with 8% chromium there is a preferred diffusion on the grain boundaries in the matrix. This is particularly evident after the sample has been etched with Nital at 5% (Fig. 9). The boride (Fe, Cr)B is present in the form of a more compact layer in alloys with a higher chromium content (18%). The micrograph shows the separation surface between the phases (Fe, Cr)B and $(Fe, Cr)_2B$.

The high chromium concentration causes boron penetration with an advance front almost parallel with the outer edge of the specimen. On the basis of the results obtained with roentgenographic analysis, we can say that the crystals of the two borides grew in such a way that they showed a markedly preferred orientation.

Figs. 10 and 11 report the variation in the percentage of chromium in the borided layer against the depth for the Fe–Cr alloys containing, respectively, 8 and 18% of this element.

The chromium level determined in the layer $(Fe, Cr)_2B$ of the Fe–Cr alloy with 18% of this element is in the order of 19%. Since at 1173 K (900° C) the maximum solubility of chromium in the tetragonal boride Fe_2B is 15% it must be foreseen that in this layer there are also components of the solid solution obtained by Cr–Fe substitution in the boride γ-Cr_2B (rhombic) [2].

In the diffraction pattern of the layer $(Fe, Cr)_2B$ a not very marked peak is observed, which is attributable to the (0 0 2) type planes of the phase γ-$(Cr, Fe)_2B$.

Figs 12 and 13 indicate the variation in chromium

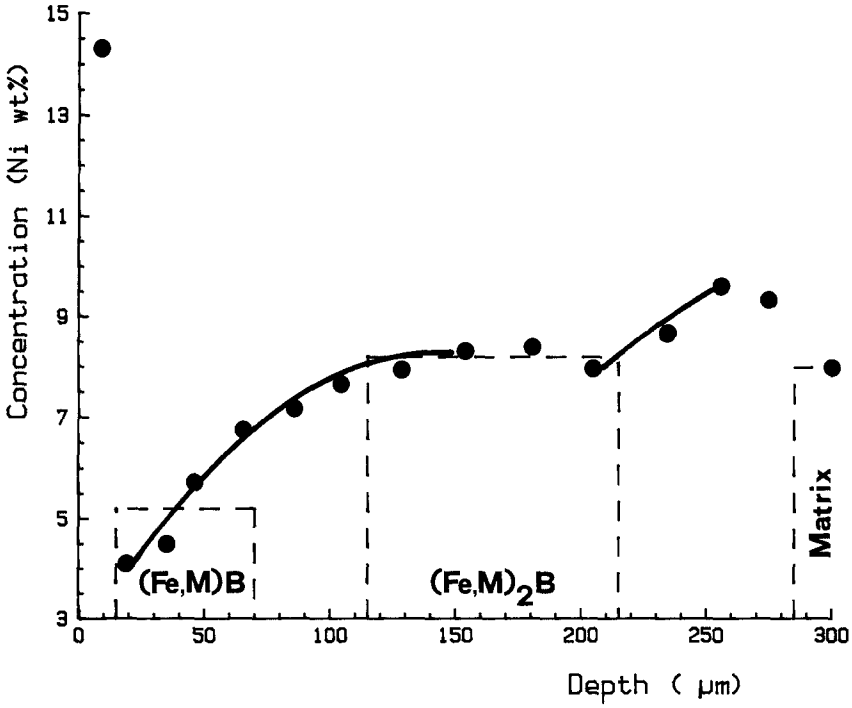

Figure 3 Fe–Ni alloy containing 8% nickel, sample No. 3: average concentration and nickel concentration profiles against depth.

and nickel concentration with depth for the Fe–Cr–Ni alloy containing 18% chromium and 8% nickel. The borided layer which is not very thick, contains predominantly the phase (Fe, Cr, Ni)B with strongly iso-oriented crystals.

The separation surfaces (Fe, M)B/(Fe, $M)_2B$ and (Fe, $M)_2B$/matrix are clear with a straight trend parallel to the edge of the specimen (Fig. 14).

Fig. 15 shows the presence of borides on the grain boundaries in the matrix.

Figs. 16 and 17 record the variations in chromium and nickel concentration on samples Fe–Cr and Fe–Ni, respectively, borided in such conditions that it was possible to obtain a one-phase diffusion layer composed of (Fe, $M)_2B$.

The distribution of the elements in the alloy between the matrix and the borided layer shows an accumulation of chromium and a depletion of nickel in the latter.

The absence of carbon and consequently of an intermediate area of boron carbides makes it possible to evaluate the distribution more clearly than is possible when operating on alloy steels [6]. In addition the absence of the phase (Fe, M)B ensures that the distribution between matrix and (Fe, $M)_2B$ is not influenced by other solubility equilibria.

The micrographic aspect of the diffusion layer of these samples is represented in Figs. 18 and 19.

4. Evaluation of the distribution ratio

The quantitative aspect of chromium and nickel distribution between the phases (Fe, M)B and (Fe, $M)_2B$ is defined by the distribution ratio proposed by Hägg and Kiessling [15] like the quotient between the atomic fractions of the atoms in the alloy:

$$\alpha_2^{Cr} = X_{Cr}^{(Fe,M)_2B} / X_{Cr}^{(Fe,M)B}$$

and

$$\alpha_1^{Ni} = X_{Ni}^{(Fe,M)B} / X_{Ni}^{(Fe,M)_2B}$$

(see their paper for further details). By the notation $X_M^{(Fe,M)_2B}$ the fraction of the M-type atoms in the phase (Fe, $M)_2B$ is meant.

The study of the systems Fe–Cr–B [10] and Fe–Ni–B [4], carried out on powder samples enabled us to obtain two curves, representing the variation of

Figure 4 Sample No. 5, not etched, 350X.

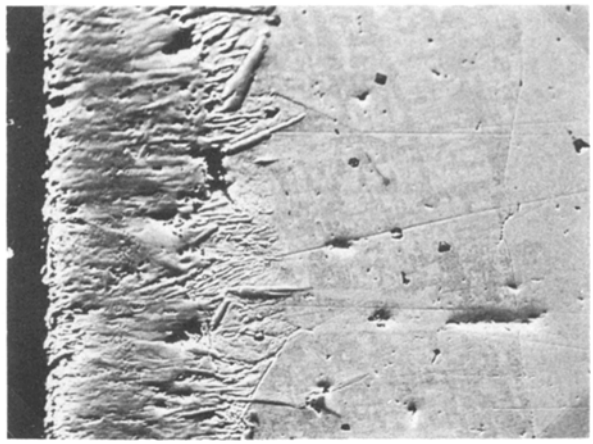

Figure 5 Sample No. 5, etched with Nital at 5%, 350X.

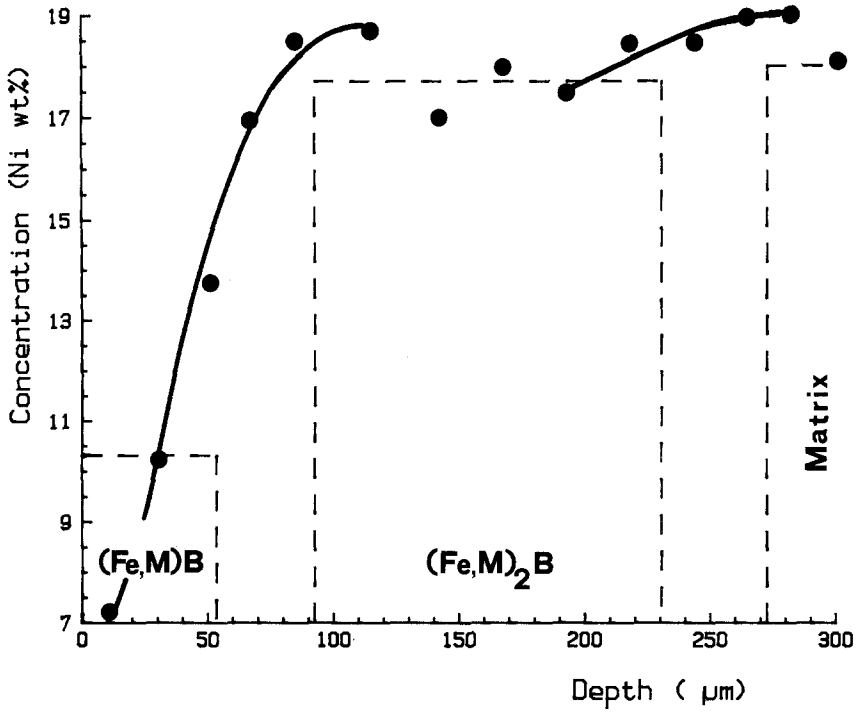

Figure 6 Fe–Ni alloy containing 18% nickel, sample No. 6: average concentration and nickel concentration profiles against depth.

α with the average atomic fraction, reported with a continuous line in Figs. 20 and 21, respectively. These figures also show the values of α_2^{Cr} and α_1^{Ni} obtained on steels with a low carbon content, AISI 430 and AISI 304 [6] and on the synthetic alloys prepared for this research.

From the examination of Figs. 20 and 21, it can be seen that the values of α_2^{Cr} and α_1^{Ni} determined on steels and on synthetic Fe–Cr and Fe–Ni alloys, are systematically greater than those defined for samples of powders (continuous line).

The fact that the α-values obtained do not coincide perfectly with the equilibrium ones can in part be attributed to the dynamics of the boron diffusion process which does not make it possible to obtain equilibrium conditions for the alloys treated like those achieved on powder samples. In addition the analytical determinations carried out passing through the two-phase zone from the boride (Fe, M)B to the (Fe, $M)_2B$ one make it possible to record a variation in concentration which does not depend only on the effective composition of the two solid solutions but also on their relative abundance.

5. Influence of the chemical composition on the hardness of the borided layers

Several authors report Vickers microhardness measurements carried out on the phases (Fe, M)B and (Fe, $M)_2B$ which constitute the layers obtained by boriding alloy steels (1, 14, 16, 17). Galibois *et al.* [16], for example, attribute Vickers microhardness values of, respectively, 2250 and 1980 $kg\,mm^{-2}$ to these phases, obtained by treating AISI C1095 steel (0.97% carbon and 0.47% manganese).

The same authors also observe that the hardness of the layers can also be influenced by physical characteristics: indeed the low value found for the borided layer in proximity of the surface, instead of the one theoretically to be expected, is explained by the presence of considerable porosity. The difference in values reported in literature [14] can be explained by a number of factors: the fact that the hardness depends on the physical characteristics of the layer and therefore on the methods of sample preparation, the different composition of samples and the difficulty

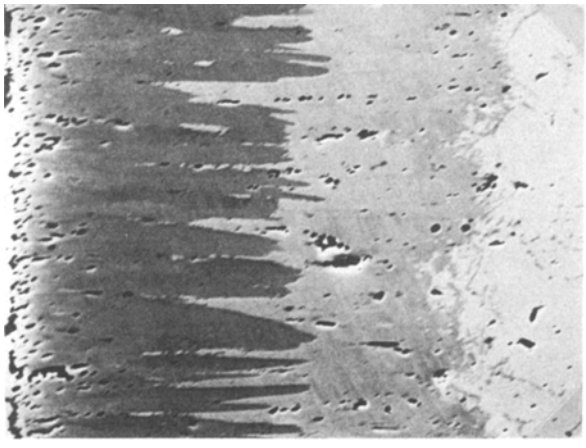

Figure 7 Sample No. 7, not etched, 700X.

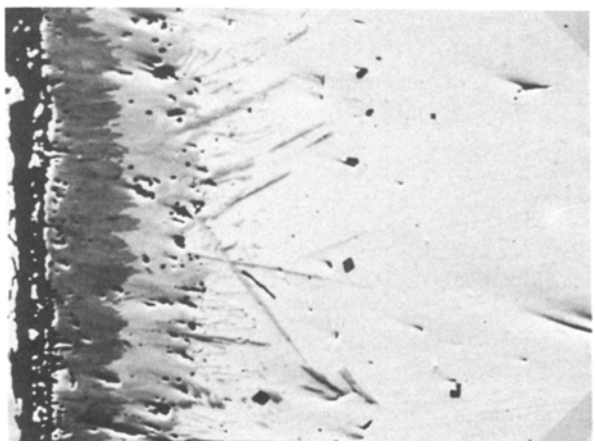

Figure 8 Sample No. 9, not etched, 350X.

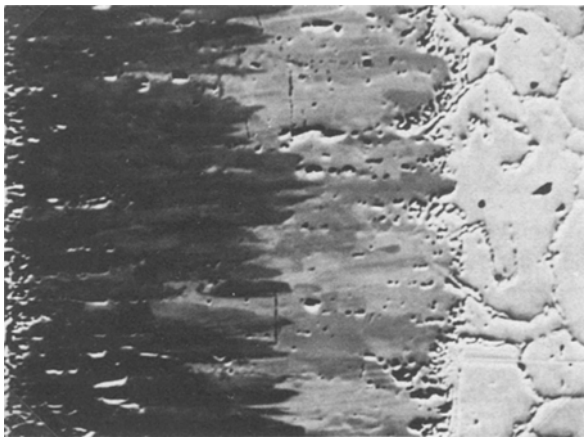

Figure 9 Sample No. 7, etched with nital at 5%, 700X.

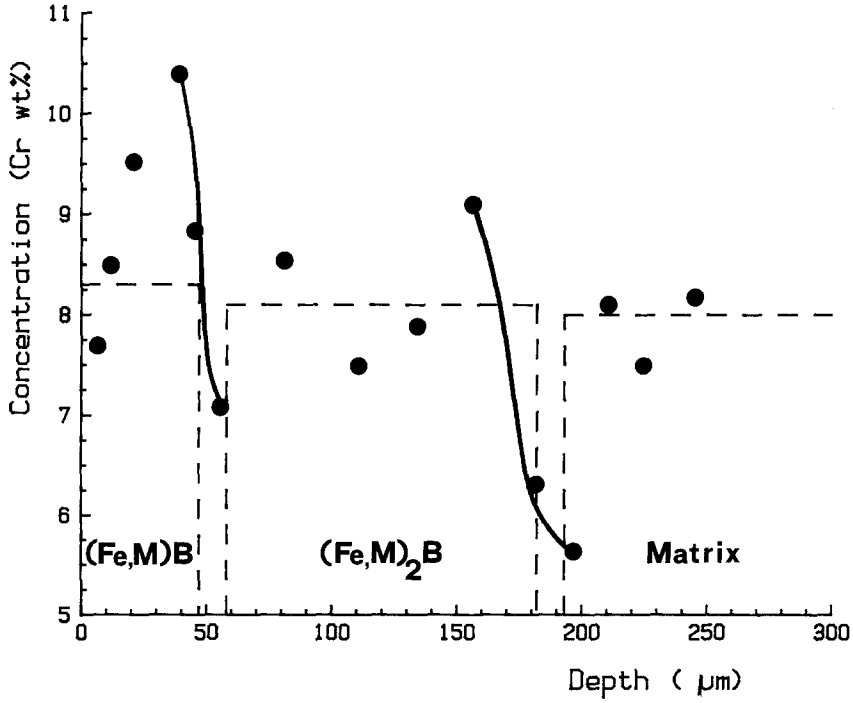

Figure 10 Fe–Cr alloy containing 8% chromium, sample No. 7: average concentration and chromium concentration profiles against depth.

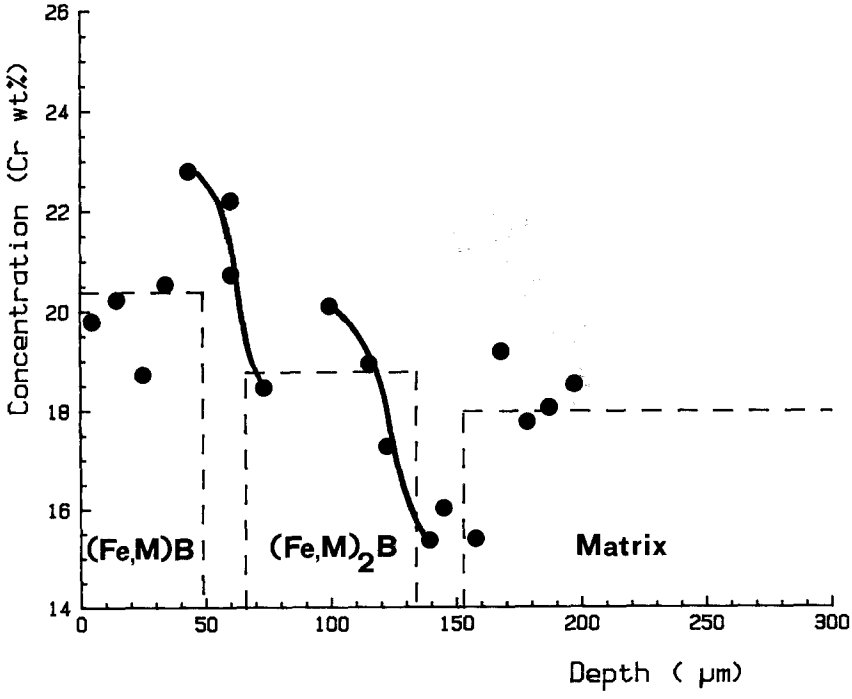

Figure 11 Fe–Cr alloy containing 18% chromium, sample No. 10: average concentration and chromium concentration profiles against depth.

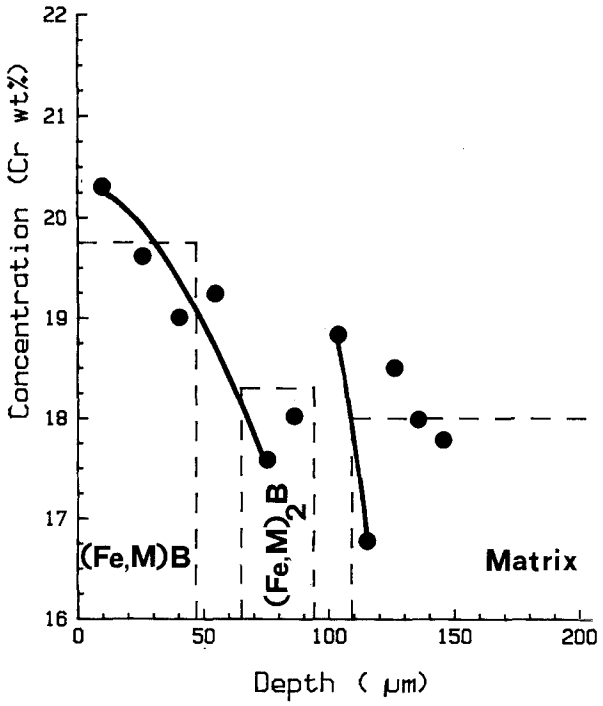

Figure 12 Fe–Cr–Ni alloy containing 18% chromium and 8% nickel, sample No. 12: average concentration and chromium concentration profiles against depth.

in carrying out measurements because of the very small dimensions and the fragility of the layer.

It was possible to ascertain that the chemical composition of the phases which constitute the borided layer although influenced as regards the metallic atom content by the distribution phenomena which we have discussed up to now, has considerable importance in determining the hardness of the layers.

The Vickers microhardness of phases FeB and Fe_2B determined as an average of numerous measurements carried out on a borided sample of Armco iron, were

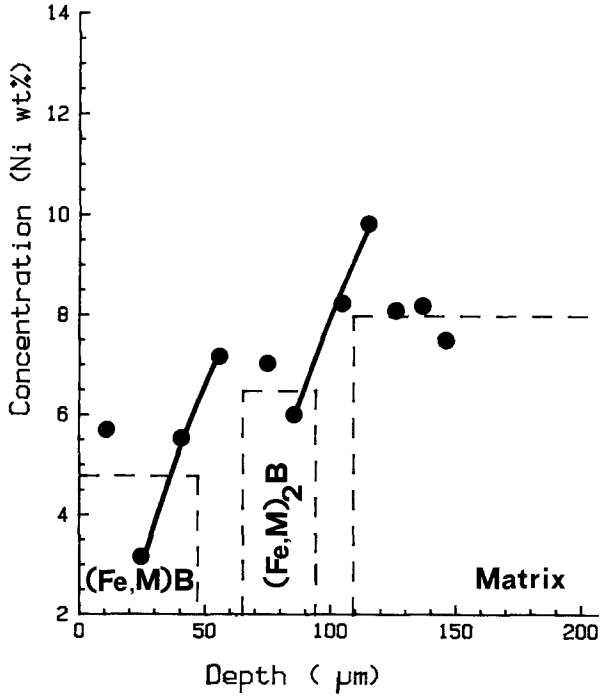

Figure 13 Fe–Cr–Ni alloy containing 18% chromium and 8% nickel, sample No. 12: average concentration and nickel concentration profiles against depth.

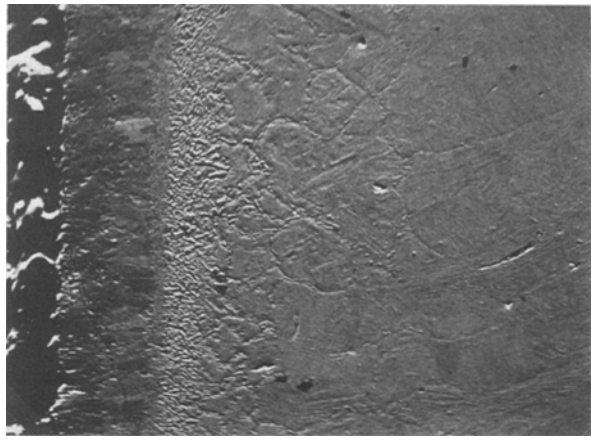

Figure 14 Sample No. 11, etched with Nital at 5%, 350X.

respectively 17.6 and 15.3 $kN\,mm^{-2}$. These values are not different from those we observed for the corresponding phases of composition (Fe, Ni)B and $(Fe, Ni)_2B$ formed after boriding an Fe–Ni alloy containing 18% nickel. On a synthetic Fe–Cr alloy with 18% chromium, however, we found microhardness of 21.2 $kN\,mm^{-2}$ for the phase (Fe, Cr)B and of 17.2 $kN\,mm^{-2}$ for that of composition $(Fe, Cr)_2B$.

Therefore, in the phases FeB and Fe_2B Fe–Cr substitution causes an increase in hardness, further accentuated by the accumulation of chromium in the diffusion layer.

Taking up the considerations of Schouler *et al.* [18] the above-mentioned increase can be explained considering the notable strength of M–M bonds, which are believed to determine the mechanical characteristics of borides with an atomic boron–metal ratio equal to or less than 1.

In addition, it is reasonable to believe that the chromium present in the borides, having an atomic radius significantly higher than iron, is capable of causing a distortion of the crystal lattice of the phases (Fe, Cr)B and $(Fe, Cr)_2B$ with a consequent increase in hardness.

The measurements carried out on samples FeB and Fe_2B and on the phases $(Fe_{0.75}Ni_{0.25})B$ and $(Fe_{0.75}Ni_{0.25})_2B$, which we prepared from powders, indicate that Fe–Ni substitution causes a slight reduction in microhardness. Therefore nickel, which to a

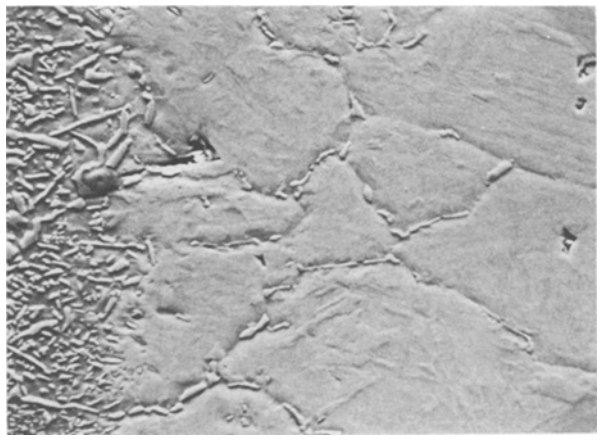

Figure 15 Sample No. 11, etched with Nital at 5%, formation of borides at the grain boundaries of the matrix, 1050X.

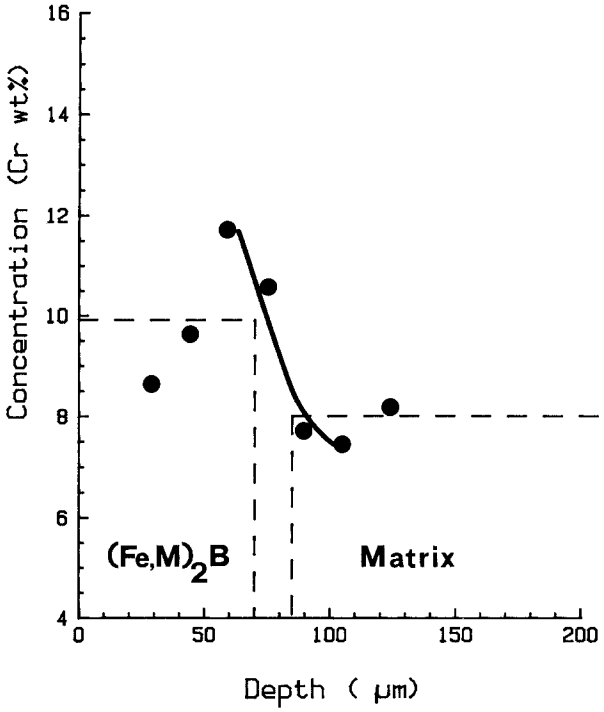

Figure 16 Fe–Cr alloy containing 8% chromium, sample No. 8: average concentration and chromium concentration profiles against depth.

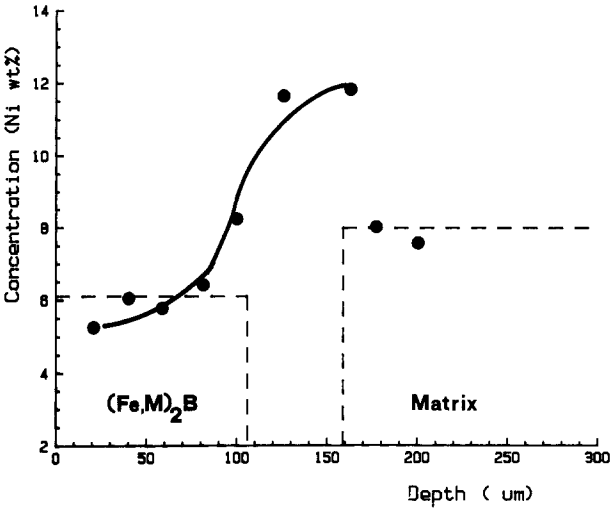

Figure 17 Fe–Ni alloy containing 8% nickel, sample No. 4: average concentration and nickel concentration profiles against depth.

Figure 18 Sample No. 4, not etched, 350X.

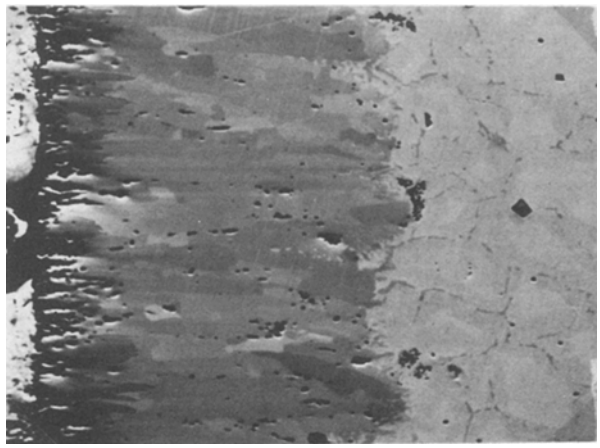

Figure 19 Sample No. 8, not etched, 700X.

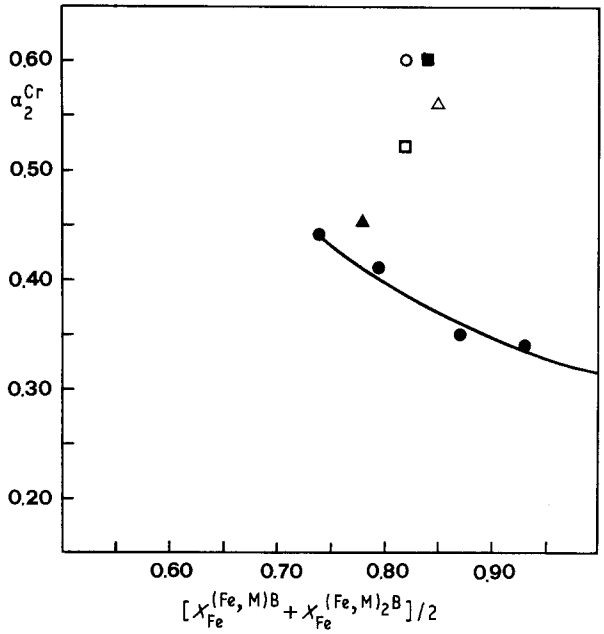

Figure 20 Chromium Hägg's distribution ratio between the phases (Fe, M)B and (Fe, M)$_2$B. The values regarding steels were calculated from the results reported by Badini *et al.* [6]. (●) Equilibrium values, (○) Fe–Cr alloy, sample 7, (□) Fe–Cr alloy, sample 10, (△) Fe–Cr–Ni alloy, sample 12, (■) AISI 430 steel, (▲) AISI 304 steel.

large extent moves away from the surface layer, has no appreciable effect on the hardness of the borided layer.

6. Conclusions

On the basis of what has been ascertained in experiments during this research we can draw the following, most significant, conclusions.

The chemical composition of the alloys subjected to treatment has a marked influence on the thickness and morphology of the diffusion layer, and also on the relative abundance of the two phases (Fe, M)B and (Fe, M)$_2$B which constitute it (M = Cr, Ni).

With the increase in nickel content the overall thickness of the layer decreases. The interfaces between different phases remain highly irregular to the variation in nickel content in the metallic alloy.

From the analysis of the diffraction patterns it seems clear that the crystals grow directing themselves

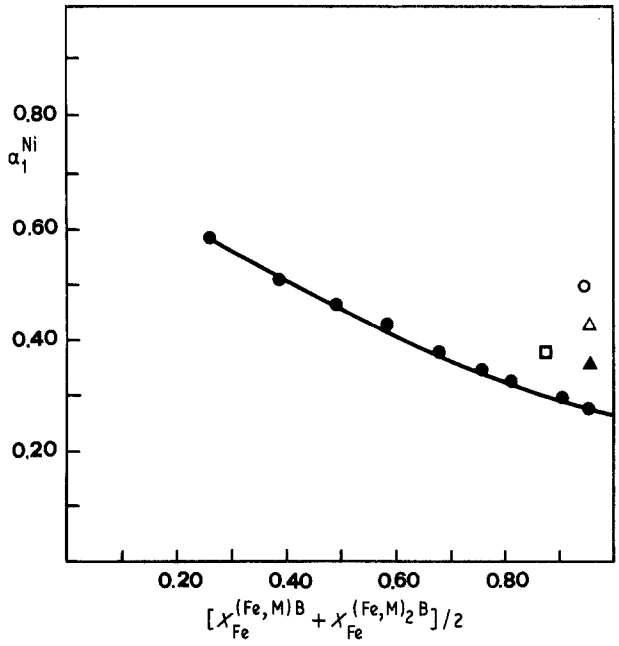

Figure 21 Nickel Hägg's distribution ratio between the phases (Fe, M)B and (Fe, M)$_2$B. The value regarding steel was calculated from the results reported earlier [6]. (●) Equilibrium values, (○) Fe–Ni alloy, sample 3, (□) Fe–Ni alloy, sample 6, (△) Fe–Cr–Ni alloy, sample 12, (▲) AISI 304 steel.

preferentially with the z-axes in a parallel direction to that of boron diffusion. This phenomenon is attenuated for samples with a higher nickel content.

In the Fe–Ni samples examined we see a greater thickness of the phase (Fe, Ni)$_2$B compared with that of the layer of (Fe, Ni)B.

The presence of chromium in the alloys brings about a greater reduction of the layer as a whole than is seen in samples containing an equal concentration of nickel.

As the chromium content increases the interfaces become more regular. In all the chromium samples examined a very strong preferred orientation was found, even more marked than that observed for Armco iron samples.

The borided layer was formed predominantly of the phase (Fe, Cr)B in the working conditions adopted.

When carbon is absent in the basic material so is the intermediate area of accumulation of carbides and/or boron carbides which was found in alloy steels. This consequently enables us to evaluate more correctly the differentiated chromium and nickel distribution, not only at the matrix/(Fe, M)$_2$B interface but also between the phases (Fe, M)$_2$B and (Fe, M)B.

The Hägg distribution ratio values found do not differ significantly from those obtained at 1173 K on Fe–Cr–B powder samples and even less from those calculated on analogous Fe–Ni–B samples.

The values observed on alloys submitted to boriding are constantly higher than the theoretical ones because of the operative conditions used in this thermochemical treatment which in any case do not allow a state of equilibrium to be reached.

The hardness of the phases (Fe, M)B and Fe, M)$_2$ is influenced differently by the presence of chromium and nickel in the basic material. Whereas nickel, present in modest concentrations in borides, does not appreciably condition the hardness of the diffusion layer, chromium brings about a considerable increase in the layer's hardness.

References

1. A. GALIBOIS, O. BOUTENKO and B. VOYZELLE, *Acta Metall.* **28** (1980) 1753.
2. C. GIANOGLIO, G. PRADELLI and M. VALLINO, *Met. Sci. Technol.* **1** (1983) 51.
3. G. PARADELLI and C. GIANOGLIO, *Atti Accad. Naz. Lincei* **57** (1975) 29.
4. C. GIANOGLIO and C. BADINI, to be published.
5. C. GIANOGLIO and E. QUADRINI, *Atti Accad. Sci. Torino* **114** (1980) 125.
6. C. BADINI, C. GIANOGLIO and G. PRADELLI, *Met. Sci. Technol.* **3** (1985) 10.
7. G. V. ZEMSKOV, R. L. KOGAN, I. M. SHEVCHENKO, E. V. KOSS, D. L. YAMROZ, P. I. GRANKIN and A. S. MATVEEVA, *Izv. Vyssh. Uchebn. Zaved. Chern. Metall.* **1** (1983) 123.
8. P. CASADESUS, C. FRANTZ and M. GANTOIS, *Mem. Sci. Rev. Mét.* **76** (1979) 9.
9. Z. JIANG, L. ZHANG, L. LI, X. PEI and T. LI, *Trans. Met. Heat Treat.* **2** (1981) 46.
10. C. GIANOGLIO and G. PRADELLI, *Atti Accad. Sci. Torino* **116** (1983) 16.
11. G. PRADELLI and C. GIANOGLIO, Atti 1° Convegno ASMI Milano 21–27 Ott. 1983 (Pitagora, Bologna, 1983) p. 143.
12. M. CARBUCICCHIO, G. MEAZZA and G. PALOMBARINI, *J. Mater. Sci.* **17** (1982) 3123.
13. P. GOEURIOT, R. FILLIT, F. THEVENOT, J. H. DRIVER and H. BRUYAS, *Mater. Sci. Engng.* **55** (1982) 9.
14. L. MARCHESINI and G. SCARINCI, *Tecn. Ital.* **36** (1971) 341.
15. G. HÄGG and R. KIESSLING, *J. Inst. Metals* **81** (1952) 51.
16. A. GALIBOIS, O. BOUTENKO and B. VOYZELLE, *Acta Metall.* **28** (1980) 1765.
17. A. N. MINKEVITCH, *Rev. Mét.* (1963) 807.
18. M. C. SCHOULER, M. DUCARROIR and C. BERNARD, *Rev. Int. Hautes Tempér. Réfract. Fr.* **20** (1983) 261.

Received 24 June
and accepted 10 July 1985